

PROCEEDINGS OF SPIE

SPIDigitalLibrary.org/conference-proceedings-of-spie

Three-dimensional imaging of human teeth: an in vitro study of caries detection using micro computed tomography

Andrés Izquierdo, Christine Tanner, Georg Schulz, Jeannette von Jackowski, Griffin Rodgers, et al.

Andrés Izquierdo, Christine Tanner, Georg Schulz, Jeannette A. von Jackowski, Griffin Rodgers, Hans Deyhle, Bert Müller, "Three-dimensional imaging of human teeth: an in vitro study of caries detection using micro computed tomography," Proc. SPIE 12242, Developments in X-Ray Tomography XIV, 122421P (10 November 2022); doi: 10.1117/12.2635624

SPIE.

Event: SPIE Optical Engineering + Applications, 2022, San Diego, California, United States

Three-dimensional imaging of human teeth - an *in vitro* study of caries detection using micro computed tomography

Andrés Izquierdo*, Christine Tanner*, Georg Schulz, Jeannette A. von Jackowski, Griffin Rodgers, Hans Deyhle, and Bert Müller

Biomaterials Science Center, Department of Biomedical Engineering, University of Basel, Gewerbestrasse 14, 4123 Allschwil, Switzerland

Biomaterials Science Center, Department of Clinical Research, University Hospital Basel, Schanzenstrasse 55, 4051 Basel, Switzerland

ABSTRACT

Caries is detected visually, often supported by palpation and conventional radiographs, and is characterized by reduced X-ray absorption. The fringe regions of carious lesions, however, are hardly distinguished. Therefore, the treatment is usually suboptimal, because either a substantial part of healthy crown is removed or the carious lesion is still partially present. This *in vitro* study applied conventional micro computed tomography to quantify remaining carious tissue after treatment with respect to the volume of tissue mechanically removed. For this purpose, 16 teeth with 23 lesions were treated by an experienced dentist. The teeth were imaged before and after caries removal using a SKYSCAN 1275 system, Bruker, Belgium. Pre- and post-treatment datasets were rigidly registered. Manual segmentation gave rise to the volume of the remaining carious tissue. Twenty of the 23 lesions had a residual carious lesion that amounted to less than 3% of the mechanically erased tissue. Still, residual caries with volumes between 0.8 and 3.4 mm³ was found in three cases. Thus, more detailed microtomography studies are to be performed to give the desired feedback for caries therapy to clinicians.

Keywords: Dentin, carious lesions, three-dimensional registration, segmentation, student course, mechanical caries removal, radiographic caries detection, hard X-ray tomography

1. INTRODUCTION

Dental caries is the most frequent human disease worldwide [1]. The dental professional can not only suitably treat caries in an advanced stage, but also detect carious lesions during their development. After faithful diagnosis, the affected hard tissues, *i.e.* enamel and dentin, are mechanically removed. Unfortunately, in most cases, healthy tissues have to be removed as well. To reconstruct the tooth, dental fillings can be placed. Function is the primary focus, but esthetics as well as costs are essential. Students at dental schools acquire the necessary knowledge to treat carious lesions stepwise. They (i) use models, (ii) practice on extracted human teeth, and (iii) treat patients - already during their education. An in-depth understanding of the procedures including the handling of the numerous dental materials is a crucial prerequisite.

There is a trend to implement digital techniques into the daily procedures of well-equipped dental offices. Radiology beyond the conventional radiography has become increasingly important for diagnosis and treatment planning as well as to validate the clinical success. The quality of volumetric data, however, is limited because of the dose issues. Fortunately, the dose issue does not apply for *in vitro* studies using extracted teeth. Consequently, micro computed tomography, well established in materials science, can be employed to detect minor differences in mineralization as caused by caries in the transition zone to healthy dentin and enamel. Similarly, the dental filling can be evaluated.

The subject of caries treatments is also part of the course «Digital Dentistry» for the Master students in biomedical engineering at the Medical Faculty of the University of Basel, Switzerland. The students become familiar with the tooth anatomy and nomenclature. They acquire knowledge of state-of-the-art dental materials and technologies. The quantitative characterization of the teeth before and after treatment by means of dental radiology and oral scanners [2] is also important. The students understand the digital workflow introduced in dental offices and learn to efficiently communicate with dentists and appreciate how to tackle challenges in dental research.

*Andres.Izquierdo@unibas.ch and Christine.Tanner@unibas.ch; phone +41 61 2075430; www.bmc.unibas.ch

A critical prerequisite for the successful therapy of a caries-affected tooth is the complete removal of carious tissue present within enamel and dentin. In dental practice, the caries is detected by tactile and visual examinations. Visual detection can be enhanced by suitable stains [3]. X rays as used for decades allow for the visualization of caries lesions in projected view. Radiographic caries detection is only suitable for detecting advanced lesions and has limited risks for false positive diagnoses [4]. As a consequence, dentists often remove more tissue than required.

This *in vitro* study is based on extracted human teeth, which exhibit naturally formed carious lesions. These teeth were three-dimensionally characterized by micro computed tomography. The imaging procedures were repeated after the mechanical removal of the carious tissue and subsequent to the filling placement. As the result of this approach, three datasets of each tooth became available for individual and combined evaluation. The treatments were performed by an experienced dentist with a rate of around 400 dental fillings per year, so that the results should be representative of the current state of the art. If any deficiency could be detected, the study may support a modification of the currently performed caries treatments.

2. MATERIALS AND METHODS

2.1 Extracted human teeth

Sixteen upper and lower incisors, canines, premolars and molars were extracted during clinical interventions. The majority of the teeth had to be removed for periodontal reasons. The decision for tooth extraction was based on the patient's medical history and in connection with the current state of health. As a result, we were able to examine freshly extracted teeth with quota of caries, but so far untreated, see the example in Fig. 1. Photographs of all teeth are available. The teeth were cleaned with an ultrasonic hand piece, and remaining soft tissue was removed. They were put in water, before they were transferred to phosphate buffered saline for storage.

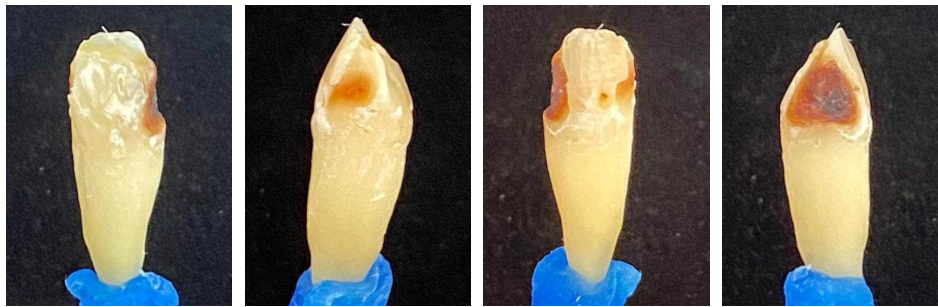


Figure 1. Photographs of the upper right canine, *i.e.* tooth 13, represented from four directions, exhibit two lesions given by the brown color.

2.2 Caries excavation

Prior to tooth preparation, radiographs for caries detection of lateral or occlusal lesions of each tooth were obtained *ex vivo* with the VistaScan Mini, Dürr Dental, Oberhasli, Switzerland. The acceleration voltage was set to 65 kV, the beam current to 8.25 mA, and the exposure time to 0.2 s. Such dental radiographs are an important adjunctive tool for caries diagnosis [5]. Two characteristic examples are given in the first column of Fig. 2.

The preparation of the caries-affected teeth occurred with diamond burs and followed the principles of tooth preparation depending on the location of the decay. The type of preparation also depended on the desired filling material and the related technique. Each tooth showed one to three independent preparation areas. Therefore, 23 areas were defined for the 16 teeth.

Caries detection was monitored using the visual-tactile method [6-8] and a caries disclosing agent (Caries Detector, Kuraray Noritake, Hattersheim, Germany) [3]. Caries detector dyes aid in caries diagnosis by staining the organic components of less mineralized, *i.e.* bacteria-infected, dentin. Tungsten steel dental burs were used for the excavation of the decalcified and infected dentin layer. Again, radiographs of lateral or occlusal lesions after removal were obtained *ex vivo* for each tooth, as exemplarily shown in Fig. 2.

2.3 Micro computed tomography

The microtomography data sets of the 16 teeth were acquired with the conventional laboratory-based system Skyscan 1275, Bruker, Kontich, Belgium - both before and after caries removal. Depending on the tooth size, the selected acceleration voltage U ranged from 60 to 75 kV and beam currents I from 133 to 166 μA . To increase the mean photon energy and to minimize the beam hardening artefacts, we incorporated 1.1 mm-thin aluminum or brass filters. The pixel size s was between 9 and 13 μm . The radiographs were acquired along 360° with angular steps a between 0.20° and 0.60° . Using exposure times t between 0.075 and 3.700 s and three to nine averages per rotation step, the total scan time T was between 15 and 355 minutes. The selected acquisition parameters for each individual dataset are listed in Table 1.

Table 1. Selected parameters for the recording of the tomography data. It has to be noted that the available scan time per tooth T was given by the teaching schedule. The teeth were denoted according to the standard ISO 3950, cf. number in first column.

Tooth	U / kV	I / μA	Filter	s / μm	a	t / ms	# averages	T / minutes
12_De	60	166	Al	9	0.25°	100	6	34
12_Ko	60	166	Al	9	0.25°	100	6	34
15_Lu	60	166	Al	10	0.25°	100	6	34
15_Wa	70	142	Al	10	0.25°	80	6	29
16_Mo	60	166	brass	10	0.25°	3700	4	355
18_Wi	70	142	brass	9	0.25°	1600	3	115
23_Ap	70	142	Al	10	0.50°	80	6	15
26_Ro	60	166	brass	10	0.25°	3700	4	355
38_Ju	70	142	brass	10	0.25°	1700	4	163
47_Ar	70	142	brass	10	0.50°	1600	6	115
47_Ne	70	142	brass	10	0.20°	1600	4	192
13_HN	70	142	Al	11	0.50°	85	9	19
15_PZ	75	133	Al	11	0.50°	75	9	21
18_AM	75	133	brass	13	0.60°	1100	5	55
28_HL	70	142	brass	13	0.50°	1600	6	68
46_VT	70	142	brass	13	0.50°	1600	6	68

2.4 Registration and segmentation

The tomographic images of the individual teeth before and after caries removal were rigidly registered to determine the amount and the exact location of the removed tissues. For the registration, we employed the open-source software elastix, version 5.0 [9] and used the normalized correlation coefficient as image similarity measure [10]. The registration was restricted to the crown tissues present in both datasets, *i.e.* excluding the removed dentin and enamel.

In the next step, we generated the difference of the tooth images acquired before and after tissue removal to determine the mechanically removed part. To compensate for noise-induced and streak artefacts, we first automatically segmented the difference image via Otsu's method [11] into foreground/background and second filled holes and removed components in the foreground via morphological closing and opening, respectively, using a spherical structural element of radius five pixel lengths [12]. The border region was then identified by morphological dilation using structure elements with a radius of 250 μm . For analysis, the border region was restricted to the remaining crown tissue.

For each of the 23 lesions, the residual caries in the border region was manually segmented. An experienced dentist slice-wise drew polygons in contrast-windowed images using ITK-SNAP, version 3.8.0 [13]. As caries can range over hundreds of slices, only every third to tenth slice was segmented. The manual segmentations for the selected slices were interpolated to obtain the remaining carious lesions. For this purpose, the interpolation of corresponding structures on neighboring segmented slices was based on combining their center of mass motion and their shape change. The latter was achieved by interpolating their distance maps [14] after center-of-mass alignment via translation. Many-to-one correspondences between neighboring structures were resolved via the closest center-of-mass distance. For neighboring structural features, that differed in size by more than a factor of four, the smaller one was dilated until a similar-sized overlap was reached with the larger one. This overlap was employed to define the sub-region of the larger structural feature corresponding to the smaller one.

3. RESULTS

3.1 Two- and three-dimensional hard X-ray imaging of the teeth

Figure 2 compares radiographs obtained *ex vivo* within the dental clinic with the corresponding projections acquired by microtomography. In addition, a virtual cut through the center of the tomography data is displayed. The conventional radiographs from the clinic show the anatomical details well, but their interpretation needs experience and correlation with tactile and optical feedback of the dentist. The selected projections of the tomography data exhibit similar resolution as the clinical radiography data. Nevertheless, the superior contrast is observed due to the higher photon statistics. A virtual cut through the three-dimensional data, however, enables to not only to discriminate between tissue types including dentin and enamel, but also to identify regions with reduced X-ray absorption. In the specific case, we know that the reduced X-ray absorption originates from the caries-induced demineralization of enamel and dentin.

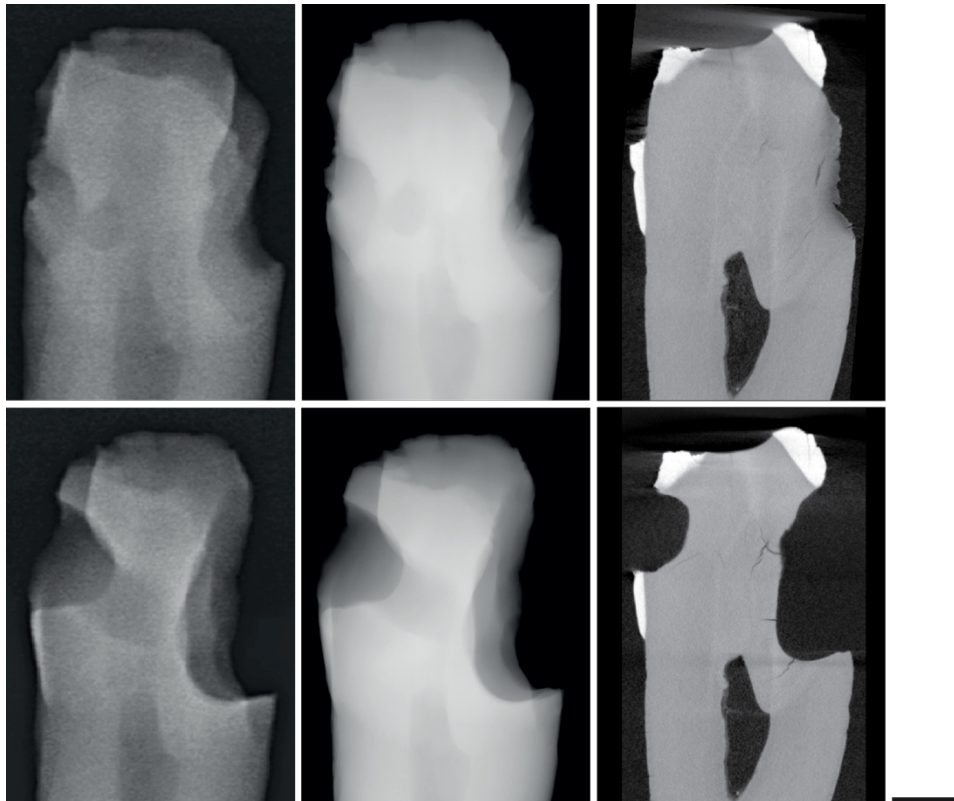


Figure 2. Radiographs and virtual slices through tooth **13** before (top row) and after (bottom row) removal of the two lesions. The images in the first column are conventional radiographs as obtained in a dental clinic. The images given in the second column show selected radiographs from the acquired tomography data. In the third column virtual cuts through the tomography data demonstrates the superior density resolution of the tomography data. The bar corresponds to a length of 2 mm and is valid for the six images.

Figure 2 contains images of the same tooth before and after removal of the carious lesion. The radiographs alone can hardly support the detection of remaining caries. The microtomography data, however, clearly show which parts of the caries-affected tooth have been mechanically removed. As virtual cuts only contain a part of the three-dimensional data, scientists and clinicians prefer a three-dimensional representation as the view of choice, as displayed in Fig. 3. Such rendering can even be obtained from truncated objects [15].

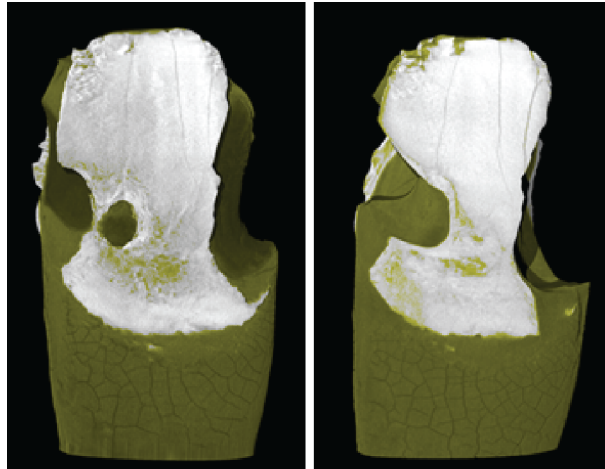


Figure 3. Three-dimensional renderings of microtomography data of tooth 13 before and after caries removal.

3.2 Detection of less dense dentin close to the removed tissue

Figure 4 exemplarily shows the rim region around the removed carious lesion, as described in Section 2.4. The selected orthogonal cuts of tooth 13 make visible the location and to a certain extent also the morphology of the carious lesion and the potential remaining caries. Whereas no remaining caries around the smaller lesion on the left was found after tissue removal, areas of lower X-ray absorption, which may be associated with caries, were detected for the larger lesion, cf. red-colored areas. An experienced dentist sparsely segmented these areas of lower X-ray absorption by hand. The resulting volumes after interpolation in relationship to the volume of the border region are listed in Table 2.

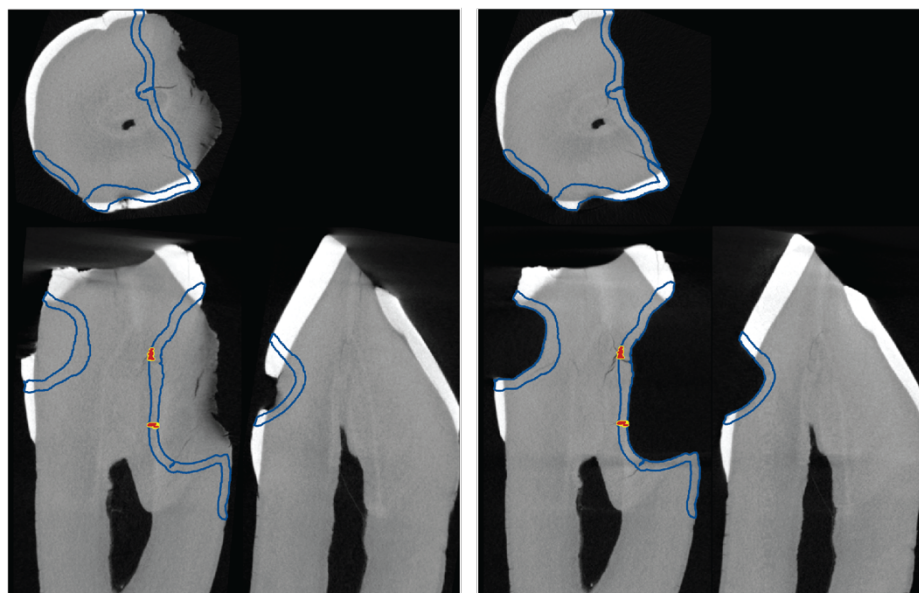


Figure 4. Three orthogonal slices of tooth 13 before (left) and after (right) mechanical lesion removal with contours depicting rim (blue), manually segmented remaining caries (red) and their interpolation (yellow).

Table 2. Volumetric analysis of demineralized dentin and enamel, which indicates remaining carious tissue. The first column contains the tooth with up to three lesions termed a to c. The second column lists the tissue volumes mechanically removed. The third column gives the volume of the 250 μm -thin border region, whereas the last two columns summarize the absolute and relative volumes of tissue in the border region potentially demineralized because of caries.

Tooth & lesion	Tissue removed / mm^3	Border region		
		Total / mm^3	Caries / mm^3	Caries / %
12_De_a	9.46	5.94	0.07	1.22
12_Ko_a	47.21	23.62	2.02	8.55
12_Ko_b	47.21	23.62	0.53	2.25
15_Lu_a	14.82	9.30	0.00	0.00
15_Lu_b	14.82	9.30	0.00	0.00
15_Wa_a	6.82	7.41	0.01	0.07
16_Mo_a	36.06	22.06	0.21	0.94
18_Wi_a	13.79	12.00	0.84	7.00
18_Wi_b	13.79	12.00	3.37	28.07
23_Ap_a	12.72	6.64	0.16	2.34
26_Ro_a	63.09	29.57	0.11	0.37
38_Ju_a	211.56	26.34	0.01	0.05
47_Ar_a	67.78	34.13	0.17	0.50
47_Ar_b	67.78	34.13	0.50	1.47
47_Ar_c	67.78	34.13	0.29	0.86
47_Ne_a	62.55	23.62	0.03	0.12
13_HN_a	39.39	19.84	0.06	0.31
13_HN_b	39.39	19.84	0.02	0.10
15_PZ_a	11.61	11.51	0.11	0.95
18_AM_a	18.35	10.51	0.10	0.95
28_HL_a	9.00	8.06	0.22	2.73
46_VT_a	13.21	9.70	0.00	0.00
46_VT_b	13.21	9.70	0.14	1.47

Obviously, an automatic segmentation of the remaining caries is challenging. To underline this statement, the absorption histograms of the removed tissue, the border region and the remaining caries are plotted in Fig. 5 for tooth **13**. Intact enamel is only present in the mechanically removed tissue and in the border region, cf. peak on the right. More important is the dentin-related main peak. The most likely value for the removed tissue (38,954) and the remaining caries (38,959) are identical within the error bars, whereas the dentin-related peak for the border region is shifted to higher X-ray absorption values (39,270). To give the reader a clearer idea on the related gray values for the tomography slices in Figs. 2 and 4 the corresponding gray-scale bar has been added on the top of the diagram. It indicates the limited number of gray values utilized for the visualization of the dentin.

It should be noted that the interpolation between every third to tenth manually segmented slice hardly influenced the histogram, cf. red- and orange-colored dots.

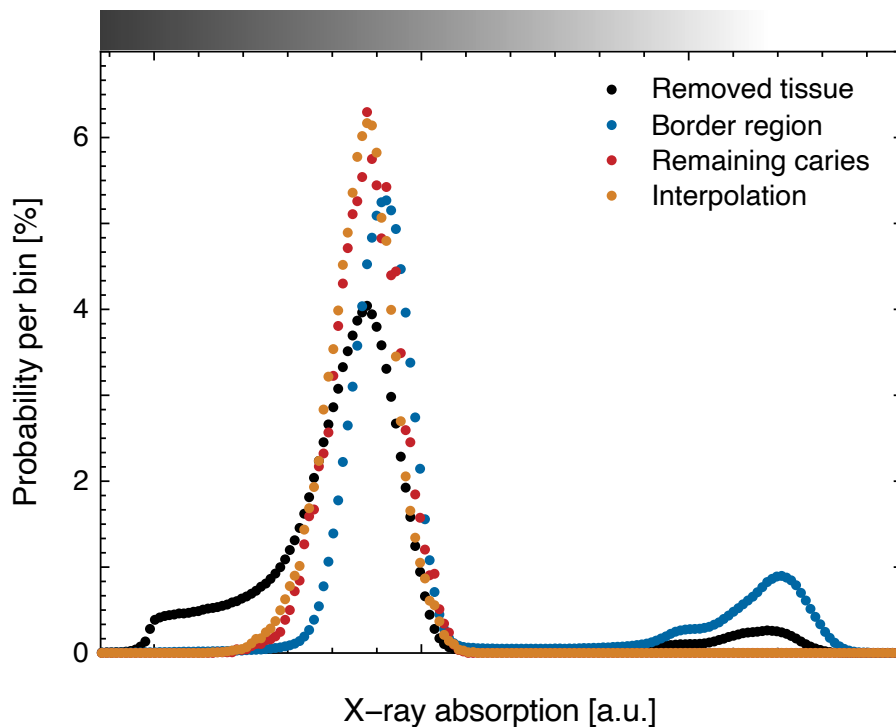


Figure 5. The histograms of measured X-ray absorption for tooth **13**: removed tissue (black dots), border region (blue dots), carious tissue for the large lesion in the rim manually segmented (red dots), and related interpolation (orange dots) demonstrate the challenge for intensity-based segmentation. The main peak is associated with dentin and the peak at larger X-ray absorption with the enamel. The grayscale corresponds to the one used for the virtual cuts in Figs. 2 and 4.

4. DISCUSSION

The study of the 16 teeth comprised two incisors from position **12**, two canines from positions **23** and **13**, three premolars from position **15** and nine molars from positions **16**, **26**, **28**, **38**, **46**, **18**, and **47**. These teeth substantially differed in size. It is a reasonable assumption that the lesion sizes correlate with the segmented rim size. Therefore, the data listed in Table 2 are regrouped and represented as vertical bar chart plots in Fig. 6.

Figure 6 contains three diagrams. The horizontal axis displays the 23 lesions of the 16 teeth ordered by decreasing volume of the rim regions. In general, the removed tissue volume decreases with decreasing rim volume, cf. top diagram. One may also expect that the remaining caries volume correlates with the size of the rim regions, which is apparently not the case, cf. central and bottom diagrams.

For three of the 23 treated lesions, we found surprisingly large volumes presenting reduced X-ray absorption within the rim region. At least for these three volumes of cubic millimeter size, the carious tissue might not have been fully excavated. Such a situation has been studied by several experts. For example, the presence of cavitations at untreated teeth, often termed the breakdown of the tooth surface, has been checked *in vitro* with the naked eye, using magnifying eyeglasses, stereo and even scanning electron microscopes [16]. The higher the magnification of the used instrument the higher is the probability to identify remaining caries after excavation [17]. Caries, remaining after mechanical treatment and filling, may cause the development of future lesions. Even lesions hardly detectable via radiography tend to progress, albeit slowly [16]. Accordingly, the entire removal of carious tissue is a fundamental part of a successful therapy. The results of this tomography-based study indicate that in certain cases carious tissue remains present even when an experienced dentist has performed the treatment outside the oral cavity. Consequently, the caries detection in dental clinics should be improved, maybe on the basis of X-ray scattering.

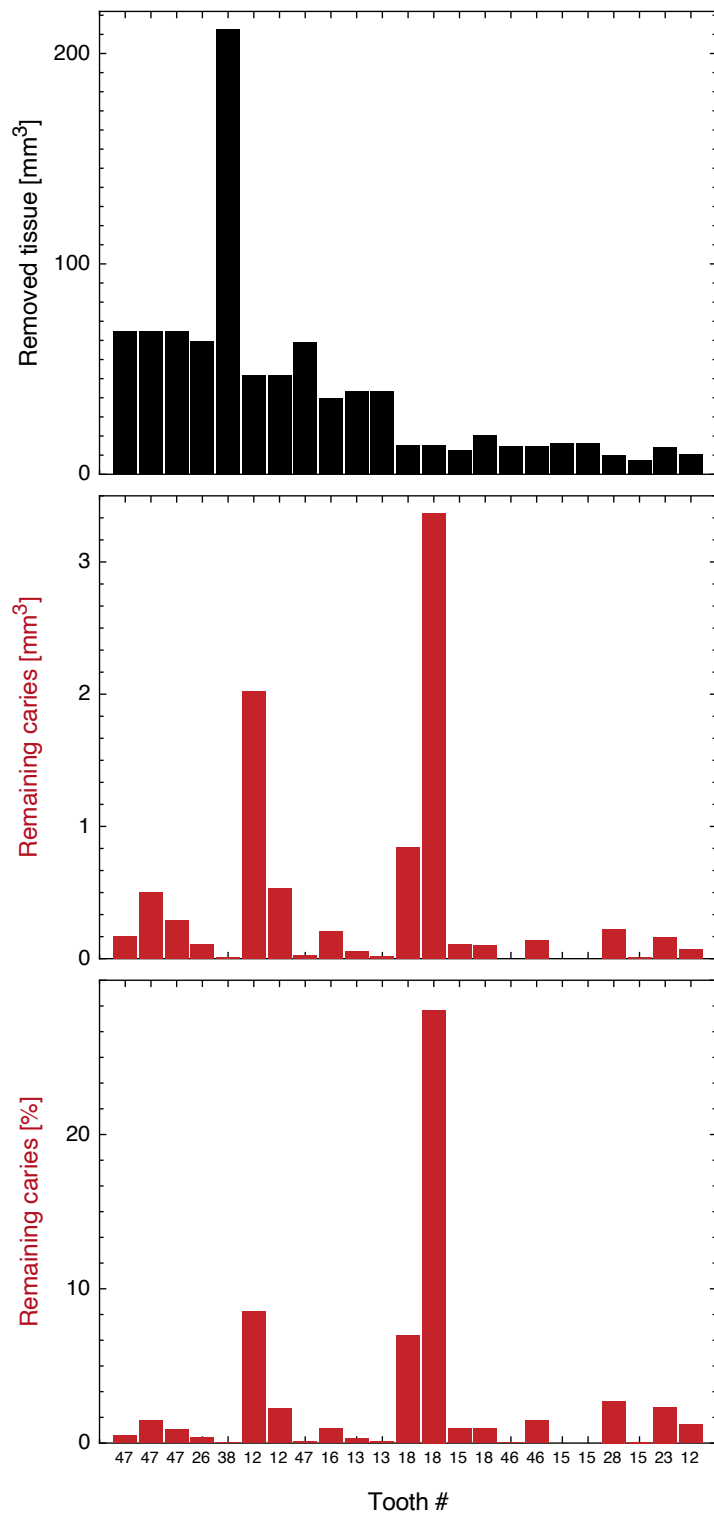


Figure 6. These vertical bar charts show the ordered size of the border region of the studied teeth on the abscissa from larger to smaller ones. The diagram on the top shows the general trend that larger lesions give rise to larger border regions. The remaining caries volume detected via X-ray absorption does not necessarily scale with the lesion or border region sizes.

Considering today's minimally invasive approaches, however, the carious lesions in the present study might be even over-prepared, *i.e.* one could keep a certain amount of demineralized dentin. Sometimes, the contemporary treatments rely on medication and fluoride releasing materials to stop the bacterial growth and to mineralize the partially demineralized dentin in addition to the mechanical removal. Pulp capping materials including mineral trioxide aggregates are used to promote remineralization of demineralized dentin [18, 19].

The goal of this tomography study was mainly focused on the education of Master students in biomedical engineering and not primarily on dental research. The caries-affected teeth were used as a medically relevant example to understand tomographic imaging in detail. After successful completion of the course «Digital Dentistry», the students are able to run the tomography system and to handle the three-dimensional data concerning visualization, segmentation, and registration.

More than a decade ago, a manuscript described the application of microtomography for teaching purposes in the field of dentistry [20]. This paper described the characterization of *in vitro* treatments of carious lesions. Although the students also acquired knowledge on the usage of a rather simple microtomography apparatus, the focus was not on the detection of remaining caries but on the careful preparation of the dental fillings.

5. CONCLUSIONS

The data listed in Table 2 and represented in Fig. 6 can be summarized as follows. For three of the 23 lesions, no indication of remaining caries could be identified. For eleven lesions, we have found less than one percent remaining caries, which might be negligible in a clinical setting. For three times each, we found values between 1 and 2 % and between 2 and 3 %, respectively. In these cases, one can anticipate an improved outcome by applying an effective dental material such as mineral trioxide aggregate. For three of the 23 lesions, however, such a treatment could be risky, because the reduced X-ray absorption indicates remaining caries with volumes of 3.4, 2.0, and 0.8 mm³, respectively. Further experiments are necessary to come to conclusive decisions on caries treatments on the basis of tomographic measurements.

Microtomography of medically relevant objects should become an important part in the curricula of Master students in a variety of fields including dentistry and biomedical engineering. This non-destructive imaging technique plays an increasing role in basic and applied research as well as industrial applications. The students should learn (i) how to prepare the objects for tomographic imaging *in vitro*, (ii) how to acquire the tomography data in an optimized fashion, (iii) how to reconstruct the data and to remove artifacts, and (iv) how to visualize and quantify the three-dimensional imaging data. Image registration to quantify the changes of the object of interest and segmentation of microstructural features belong to the essential teaching and learning contents of current Master programs. In this respect, the authors tried to actively contribute to education and training at university level.

ACKNOWLEDGEMENT

The authors thank the Master students in biomedical engineering at the Medical Faculty of the University of Basel, Switzerland, namely Julia Apaza Arpi, Arslan Aybüke, Nuria de Santiago Giner, Alp Can Gülan, Nicole Jucker, Maximilian Köhler, Bassma Lheimeur, Henna-Riikka Littunen, Friedrich Lünsmann, Adriana Manea, Dominik Mory, Adrian Müller, Karl Hendrik Ulf Neugebauer, Colino Neves, Isabella Ortiz Drada, Marc Puschmann, Bassel Rashed, Maximilian Rose, Ksenia Sovdagarova, Veronica Towianski, Regina Walther, Matthias Wiesli, Parichehr Zarean, and Paridokht Zarean for their engagement during preparative work and data acquisition.

REFERENCES

- [1] Pitts, N. B., Twetman, S., Fisher, J., and Marsh, P. D., "Understanding dental caries as a non-communicable disease," *British Dental Journal* **231**(12), 749-753 (2021).
- [2] Sacher, M., Schulz, G., Deyhle, H., Jäger, K., and Müller, B., "Accuracy of commercial intraoral scanners," *Journal of Medical Imaging* **8**(3), 035501 (2021).
- [3] McComb, D., "Caries-detector dyes--how accurate and useful are they?," *Journal of Canadian Dentistry Association* **66**(4), 195-8 (2000).

- [4] Schwendicke, F., Tzschoppe, M., and Paris, S., "Radiographic caries detection: A systematic review and meta-analysis," *Journal of Dentistry* **43**(8), 924-33 (2015).
- [5] Keenan, J. R., and Keenan, A. V., "Accuracy of dental radiographs for caries detection," *Evidence Based Dentistry* **17**(2), 43-43 (2016).
- [6] Gimenez, T., Piovesan, C., Braga, M. M., Raggio, D. P., Deery, C., Ricketts, D. N., Ekstrand, K. R., and Mendes, F. M., "Visual inspection for caries detection: A systematic review and meta-analysis," *Journal of Dental Research* **94**(7), 895-904 (2015).
- [7] Gomez, J., "Detection and diagnosis of the early caries lesion," *BMC Oral Health* **15**(1), S3 (2015).
- [8] Hoskin, E. R., and Keenan, A. V., "Can we trust visual methods alone for detecting caries in teeth?," *Evidence Based Dentistry* **17**(2), 41-2 (2016).
- [9] Klein, S., Staring, M., Murphy, K., Viergever, M. A., and Pluim, J. P., "elastix: A toolbox for intensity-based medical image registration," *IEEE Transactions in Medical Imaging* **29**(1), 196-205 (2010).
- [10] Hill, D. L., Batchelor, P. G., Holden, M., and Hawkes, D. J., "Medical image registration," *Physics in Medicine and Biology* **46**(3), R1-45 (2001).
- [11] Otsu, N., "A threshold selection method from gray-level histograms," *IEEE Transactions on Systems, Man, and Cybernetics* **9**(1), 62-66 (1979).
- [12] Haralick, R. M., Sternberg, S. R., and Zhuang, X., "Image analysis using mathematical morphology," *IEEE Transactions on Pattern Analysis and Machine Intelligence* **PAMI-9**(4), 532-550 (1987).
- [13] Yushkevich, P. A., Yang, G., and Gerig, G., "ITK-SNAP: An interactive tool for semi-automatic segmentation of multi-modality biomedical images," *Annual International Conference of the IEEE Engineering in Medicine and Biology Society* **2016**, 3342-3345 (2016).
- [14] Schenk, A., Prause, G., and Peitgen, H.-O., "Efficient semiautomatic segmentation of 3D objects in medical images," *Lecture Notes in Computer Science* **1935**, 186-195 (2000).
- [15] Deyhle, H., White, S. N., Bunk, O., Beckmann, F., and Müller, B., "Nanostructure of carious tooth enamel lesion," *Acta Biomaterialia* **10**(1), 355-64 (2014).
- [16] Kielbassa, A. M., Paris, S., Lussi, A., and Meyer-Lueckel, H., "Evaluation of cavitations in proximal caries lesions at various magnification levels in vitro," *Journal of Dentistry* **34**(10), 817-22 (2006).
- [17] Koç Vural, U., Kütük, Z. B., Ergin, E., Yalçın Çakır, F., and Gürkan, S., "Comparison of two different methods of detecting residual caries," *Restorative Dentistry & Endodontics* **42**(1), 48-53 (2017).
- [18] Hernández, M., Cobb, D., and Swift, E. J., Jr., "Current strategies in dentin remineralization," *Journal of Esthetic and Restorative Dentistry* **26**(2), 139-45 (2014).
- [19] Kim, J., Song, Y. S., Min, K. S., Kim, S. H., Koh, J. T., Lee, B. N., Chang, H. S., Hwang, I. N., Oh, W. M., and Hwang, Y. C., "Evaluation of reparative dentin formation of ProRoot MTA, Biodentine and BioAggregate using micro-CT and immunohistochemistry," *Restorative Dentistry & Endodontics* **41**(1), 29-36 (2016).
- [20] Deyhle, H., Schmidli, F., Krastl, G., and Müller, B., "Evaluating tooth restorations: Micro computed tomography in practical training for students in dentistry," *Proc. SPIE* **7804**, 780417 (2010).